Engineered Science
DOI: https://dx.doi.org/10.30919/es1504

Numerical Simulation on Impact Performance of Ceramic-Based Ultra-High Molecular Weight Polyethylene Composite Armor

Yedige Aidyn,[1] Manap Ardak,[1] Yernar Kanagat,[1,2] Aidyn Altay,[1] Bakhtiyarova Sayagul Zhaksybaevna,[3] Primbetov Azamat Auesbaevich,[4] Dilnur Tussipkan,[5] Kairat Aidarkhan,[6] Sagidolla Batay[7,*] and Ali Zhalel[1,*]

Abstract

This paper aims to investigate the anti-penetration capabilities of ceramic composite armor backed by a layered composite of Titanium Alloy Grade 5 (Ti6Al4V) and ultra-high molecular weight polyethylene (UHMWPE) against a high-velocity 12.7 mm diameter projectile traveling at 818 m/s. The study employs numerical simulations using Ansys software to analyze the bullet-proof mechanism of the entire armor system, as well as the performance of the UHMWPE layer in isolation. By focusing on the behavior of these armor layers during impact, the study provides insights into how different materials contribute to energy absorption and resistance to penetration. A key aspect of this work is the comparison between simulations using both rigid and flexible projectiles, allowing for a more comprehensive understanding of the impact dynamics. This research contributes to the broader field of armor design and impact resistance by offering a detailed analysis of the interactions between projectiles and multi-layered composite armor systems. The findings have potential applications in the development of more efficient and reliable ballistic protection systems, where material optimization and structural configuration are critical factors in enhancing performance against high-velocity threats.

Keywords: Composite armor; Alumina; Ceramics; UHMWPE.
Received: 03 November 2024; Revised: 08 January 2025; Accepted: 17 January 2025.
Article type: Research article.

1. Introduction

The study of ballistic impacts and armor designs has been a cornerstone in improving personal and vehicular protection systems against high-velocity projectiles. The development of lightweight armor systems has garnered significant attention in recent years as researchers and manufacturers strive to improve ballistic performance while reducing weight and cost. A critical component of modern composite armors is the use of advanced ceramics, which play a pivotal role in dissipating projectile energy.[1] Ceramic materials, such as alumina (Al_2O_3), silicon carbide (SiC), and boron carbide (B_4C), are highly valued for their hardness and stiffness, allowing them to blunt and fragment projectiles effectively.[2] Alumina is especially popular due to its cost-effectiveness, while silicon carbide is preferred for its performance in lightweight applications.[3]

The geometry of ceramic components is another crucial factor in determining ballistic performance. Cylindrical and hexagonal shapes are commonly used against direct gunfire due to their optimal balance of coverage and energy dissipation. Larger ceramic tiles, on the other hand, are more suitable for protection against fragments and improvised explosive devices (IEDs). The thickness of the ceramic layer varies depending on the anticipated threat level and generally ranges between 4 mm and 25 mm. Ceramics, when used as the outer strike face, excel at blunting and cracking projectiles, consuming a substantial portion of their kinetic energy through fragmentation.[4]

Complementing ceramics in composite armor systems are backing materials designed to absorb and dissipate the residual

[1] *L.N. Gumilyov Eurasian National University, Astana, 010000, Republic of Kazakhstan*
[2] *National Laboratory Astana, Astana, 010000, Republic of Kazakhstan*
[3] *West Kazakhstan University named after M. Utemisova, Uralsk, 090009, Kazakhstan*
[4] *Nukus Branch of the Uzbek State University of Physical Culture and Sports, Nukus, 230100, Republic of Karakalpakstan, Uzbekistan*
[5] *National Center for Biotechnology, Astana, 010000, Republic of Kazakhstan*
[6] *"Shipali" medical center, Astana, 010000, Republic of Kazakhstan*
[7] *Department of Intelligent Systems and Cybersecurity, Astana IT University, Astana, 010000, Republic of Kazakhstan*
**Email*: zhalel.ali.phd114@mail.ru (Z. Ali);
B.Sagidolla@astanait.edu.kz (S. Batay)

energy from impacts. Among these, ultra-high molecular weight polyethylene (UHMWPE) has emerged as a standout material due to its exceptional strength-to-weight ratio and unparalleled ballistic impact resistance compared to other fiber-reinforced plastics.[5,6] UHMWPE is the lightest fiber material currently available, making it an ideal choice for lightweight armor designs. Despite its introduction in the 1970s, UHMWPE remains widely used in modern composite systems due to its unique combination of properties.[7] Researchers have also found that UHMWPE fiber composites outperform woven fabrics in ballistic resistance, further cementing their role in advanced armor systems.

The synergy between ceramics and UHMWPE forms the foundation of many cutting-edge hybrid armor designs.[7] In such systems, the ceramic strike face disrupts the projectile, while the UHMWPE layer absorbs the residual energy, preventing penetration and minimizing damage to subsequent layers.[8] Titanium alloys like Ti6Al4V are often incorporated into these systems to provide additional structural support and enhance energy dissipation.[8,9] For example, hybrid designs featuring Ti6Al4V layers sandwiching UHMWPE have demonstrated significant improvements in ballistic performance by maintaining structural integrity and minimizing back-face deformation.[10, 11-13]

Numerous studies have validated the effectiveness of these designs through both experimental and numerical approaches. For instance, Marzena Fejedys *et al*. investigated hybrid ceramic-UHMWPE armor systems with varying ceramic shapes, thicknesses, and layer compositions.[14] They found that the material selection and geometry of the ceramic tiles significantly influence the system's ballistic resistance. Similarly, Hu *et al*. compared the performance of cylindrical, hexagonal, and square ceramic mosaics supported by UHMWPE against high-velocity projectiles.[15] Their findings highlighted the importance of interaction time between armor layers and projectiles in enhancing ballistic resistance.

Other studies have explored the benefits of UHMWPE in multi-layered systems.[16] Xin Li *et al*. compared titanium-based fiber metal laminates (FMLs) with carbon fiber-reinforced plastic (CFRP) and UHMWPE as intermediate layers.[14,10,11] Their results demonstrated that UHMWPE-based FMLs outperformed CFRP-based systems in ballistic impact performance, particularly in terms of energy dissipation and impact resistance. Additionally, Quen Wang *et al*. designed an innovative armor system comprising cylindrical alumina tiles, UHMWPE, and Ti6Al4V layers, demonstrating the effectiveness of this configuration against high-speed penetrators.[10]

Building upon these advancements, this paper aims to analyze a composite armor system featuring cylindrical ceramic strike faces and a layered backing structure of Ti6Al4V and UHMWPE. The proposed system is evaluated through numerical simulations performed in ANSYS/Explicit Dynamics, employing both rigid and deformable steel projectiles at an impact velocity of 818 m/s. The simulations aim to provide a detailed correlation with real-world impact tests, focusing on fracture mechanisms, energy dissipation, and deformation behavior. By emphasizing the critical roles of ceramics and UHMWPE in modern armor designs, this study contributes to the development of lightweight, high-performance ballistic protection systems tailored for contemporary defense needs.

2. Analysis and modeling

In this section, a short description of the armor's geometrical model and the numerical model is provided, and the models are reasoned on analytical means.

2.1 Problem definition

In this paper, firstly, a comparison between the finite element model analysis of the impact tests with either rigid or flexible projectiles (which can be deformed during the simulation instead of being rigid) is presented, and the results are discussed and contrasted with the real experiment results. Secondly, the sole UHWMPE layer's ballistic performance without other materials' support or accompaniment is simulated and analyzed.

2.2 Geometrical model

The schematic of the armor structure for the ballistic test and the analysis purpose is provided in Fig. 1. The construction is made up of a layer of ceramic cylinders of 18mm in both diameter and height, arrayed in contact with each other as a strike face.[3,8] In some of these papers, more shapes of the mosaic are analyzed and compared, including square, hexagonal, and pentagonal shapes. In addition, the cylindrical ceramics are backed by two layers of Ti6Al4V (100 mm × 100 mm × 3 mm and 100 mm × 100 mm × 2 mm, respectively) and sandwiching a layer of ultrahigh weight molecular polyethylene UHWMPE (100 mm × 100 mm × 5 mm), which was also provided and tested experimentally and numerically in Abaqus.[3,8]

2.3 Constitutive model and numerical simulation

To analyze the anti-penetration properties of the given structure and make some comparison with the previous work done by other researchers, as well as the ballistic performance of the sole UHWMPE layer, which is the middle layer of the structure being analyzed in our paper, in the same impact conditions, some numerical simulations in Ansys/explicit dynamics are implemented. Three typical cases were analyzed along with different numbers of surrounding cylindrical ceramics.[3] Nevertheless, in our simulation, Case 1 with one more surrounding ceramics layer, as shown in Fig. 1, in which the projectile impacts the cylinder at the center face-to-face directly, is investigated.

In the lightweight armor design, ceramic materials are common and usually designed for high-velocity ballistic impacts.[17,18-22] Under simple loading conditions, the ceramics may be taken as elastic-brittle materials.[23] Nevertheless, in

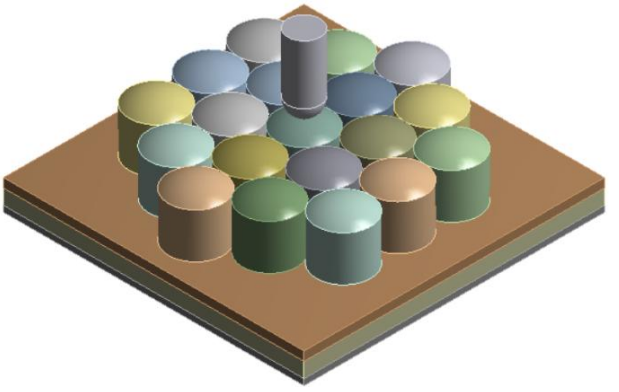

Fig.1: Impacting profile in Ansys simulation.

terms of ballistic impacts, the response of the ceramics is of importance in terms of yielding. And the JH-2 model is the most popular one for the simulation of ceramics failure. The equation depicting the response of the material is as follows, which depicts the material strength as a function of intact strength (σ_i^*), failure strength (σ_f^*), and damage (D).

$$\sigma^* = {\sigma_i}^* - D(\sigma_i^* - \sigma_f^*) \quad (1)$$

The aforementioned stresses are normalized about σ_{HEL}. As follows, $\sigma_{HEL}$is defined as the function of HEL, which is the Hugoniot elastic limit, and P_{HEL} is the pressure at the Hugoniot elastic limit. In the meanwhile, the normalized intact strength (σ_i^*), fractured strength (σ_f^*) are given in Eqs. (1)-(4), respectively, in terms of normalized pressure ($P*$) and hydrostatic pressure ($T*$) with respect to P_{HEL}.

$$\sigma_{HEL} = \frac{3}{2}(HEL - P_{HEL}) \quad (2)$$

$$\sigma_i^* = A(P^* + T^*)^N(1 + C\ ln\ \varepsilon^*) \leq \sigma_i^{max} \quad (3)$$

$$\sigma_f^* = B(P^*)^M(1 + C\ ln\ \varepsilon^*) \leq \sigma_f^{max} \quad (4)$$

$$P = K_1\mu + K_2\mu^2 + K_3\mu^3 \quad (5)$$

In Eq. (5), the Equations of state (EOS) are expressed as a function of bulk modulus (K_1), material constants (K_2, K_3), and compressibility factor (μ). To make the description of the mechanical properties of the ceramics by the JH-2 model, parameter $A, B, C, M, N, T, HEL, D_1, D_2$ must be determined.[23] Moreover, the JH-2 failure model parameters are given as in Table 1.[24]

Table 1: Mechanical properties of alumina for the JH-2 model.

Constants	Unit	Alumina
Density, ρ	kg/m³	3700
Shear modulus, G	GPa	152
Intact strength coefficient, A	-	0.93
Fracture strength coefficient, B	-	0.31
Strain rate coefficient, C	-	0.007
Intact strength exponent, N	-	0.64
Fracture strength exponent, M	-	0.6
Normalized maximum fractured strength, σf max	-	1.0
Hugoniot elastic limit, HEL	GPa	19
Pressure at HEL, PHEL	GPa	1.4
Reference strain rate, $\dot{\varepsilon}_0$	s^{-1}	1.0
Damage coefficient, D_1	-	0.001
Damage exponent, D_2	-	1.0
Bulk modulus, K_1	GPa	231
Pressure coefficient, K_2	GPa	0
Pressure coefficient, K_3	GPa	0
Bulking factor, β	-	1.0

Table 2: Mechanical properties of core steel and Ti6Al4V in the JC model.

Constants	Unit	Steel	Ti6Al4V
Density, ρ	kg/m³	7.80	4.45
Shear modulus, G	GPa	81.8	40.98
Bulk modulus, K	GPa	175	104
Static yield strength, A	GPa	1.0	1.1
Strain hardening coefficient, B	GPa	0.51	0.845
Strain hardening exponent, n	-	0.26	0.58
Strain rate coefficient, C	-	0.014	0.014
Reference Strain rate, ε_0	s^{-1}	1.0	1.0
Thermal softening exponent, m	-	1.03	0.753
Reference temperature, t_0	K	298	298
Melting temperature, t_m	K	1793	1951
Damage constant, D_1	-	0	0
Damage constant, D_2	-	0.33	0.27
Damage constant, D_3	-	-1.5	0.48
Damage constant, D_4	-	0	0.014
Damage constant, D_5	-	0	3.8

In the meantime, as shown in Table 2, the failure model of the Ti6Al4V and steel projectiles is featured by using the Johnson-Cook model, for which the determination process of the associated parameters can be found.[25] At the same time, the relevant parameters for the JH-2 and J-C models of the alumina and Ti6Al4V are given.[24]

As for the UHWMPE failure model, the orthotropic linear elastic model is utilized. The relevant parameters.[26] In numerical simulation, the steel projectile is set as either rigid or flexible to make a comparison with the results of the impact tests from both the numerical simulations and the real impact experiments on Case 1, as defined and implemented.[3,8] During the impact failure, the failed elements will be deleted automatically by default in Ansys.

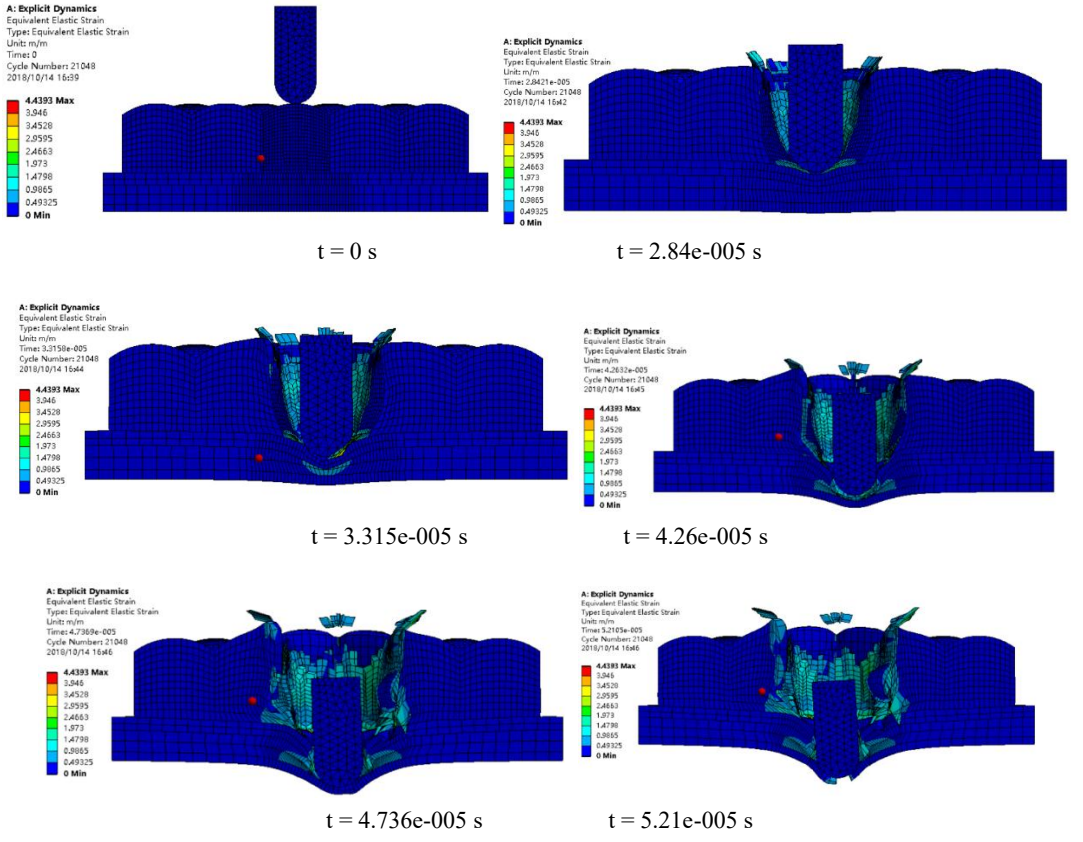

Fig.2: Armor structure failure processes on impacting against the rigid projectile in Ansys/explicit dynamics.

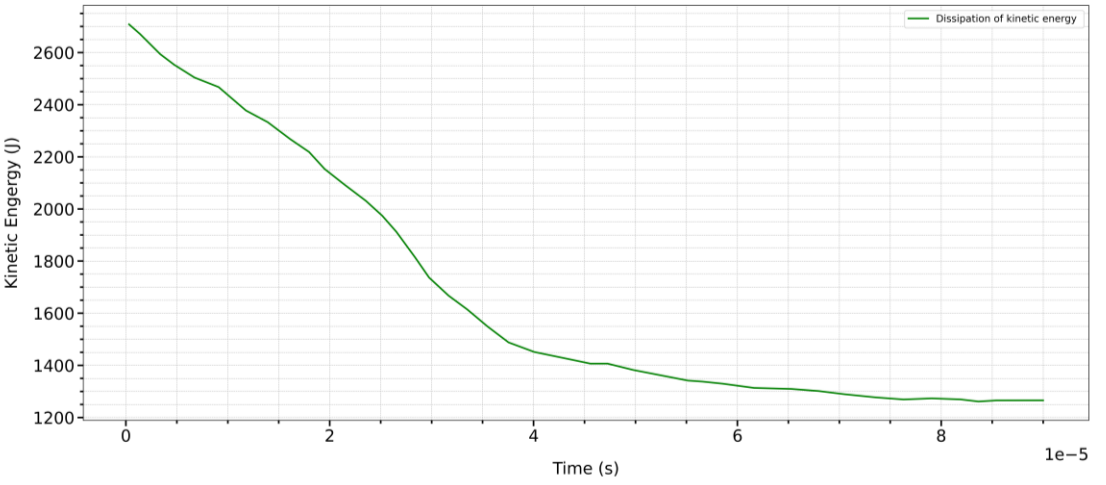

Fig. 3: Dissipation of kinetic energy of the rigid projectile during penetration.

3. Results and discussion

3.1 Simulation with rigid projectile

The penetrating processes subject to the rigid projectile are shown in Fig. 2 just for case 1, where the projectile impacts one of the ceramic cylinders perpendicularly, face to face.

Diagram which can show how the kinetic energy of rigid projectile dissipated during the penetration at different time scale is given in Fig. 3, where the initial kinetic energy (2749 J) is as much as the half of the total initial kinetic energy of the projectile as the half part of the structure is taken for simulation due to the symmetric property. During the whole anti-penetration process, half of the structure absorbed around 1452.8 J kinetic energy of the half projectile, which is equal to 53 % of the total energy. With the rest of the energy, the projectile, as a rigid one, penetrated the armor. As for the ceramic cylinder, which is penetrated fully at around 3E005 s, it accounts for about 65% of the total energy absorption, which is amazingly more or less the same as the energy absorption ratio of the ceramic cylinder layer during the penetration simulation in Abaqus.[3] While the armor was not penetrated, the rigid projectile was stopped before piercing the last layer. Owing to the erosion of the failed nodes, failure is deleted automatically. Additionally, as soon as the projectile hits the target, the wreckage of the failure blows apart around, which makes the simulation more realistic, although in the simulation, no such phenomenon took place.[27]

3.2 Simulation with flexible projectile

The study investigates the performance of various layered protective configurations against flexible bullet impacts. Each case utilizes a flexible bullet and a combination of protective materials arranged in specific layers. The configurations are:

- Case 1: Bullet, ceramic cylinders, Ti6Al4V (3 mm), UHMWPE (5 mm), Ti6Al4V (2 mm).
- Case 2: Bullet, Ti6Al4V (3 mm), UHMWPE (5 mm), Ti6Al4V (2 mm).
- Case 3: Bullet, UHMWPE (5 mm), Ti6Al4V (2 mm).
- Case 4: Bullet, UHMWPE (5 mm).

Each structure was subjected to the same flexible bullet impact, and the performance was assessed by monitoring the kinetic energy dissipation over time, as observed in the corresponding plots. Data was collected from simulations or experimental setups. And from the kinetic energy absorption in Fig. 4, we can conclude that:

Case 1 (Ceramic + Ti6Al4V + UHMWPE):

- Exhibited the highest kinetic energy dissipation rate.
- The ceramic cylinders effectively absorbed and dispersed the impact energy, protecting the underlying layers.
- Ti6Al4V layers provided structural strength, while UHMWPE contributed flexibility and energy absorption.

Case 2 (Ti6Al4V + UHMWPE):

- Demonstrated good energy dissipation but slightly less effective than Case 1.
- Without ceramic, the impact was directly distributed to Ti6Al4V, reducing its ability to sustain higher impacts over time.

Case 3 (UHMWPE + Ti6Al4V):

- Energy dissipation was lower than in Cases 1 and 2.
- The absence of the top Ti6Al4V layer reduced structural resistance to the initial impact.

Case 4 (UHMWPE only):

- The least effective in dissipating energy.
- UHMWPE alone lacked the structural reinforcement provided by Ti6Al4V or ceramic, leading to quicker energy transmission.

The results demonstrate that the inclusion of ceramic in Case 1 significantly enhances the overall impact of resistance. Ceramic provides a hard, brittle layer that breaks upon impact, dissipating energy over a wider area and preventing concentrated stress on the lower layers. The Ti6Al4V layers offer mechanical strength, while the UHMWPE adds flexibility and further absorbs energy. In Cases 2 and 3, the absence of ceramic reduces energy dissipation efficiency. Case 4 highlights the limitations of UHMWPE when used alone, emphasizing the importance of combining materials for optimal performance.

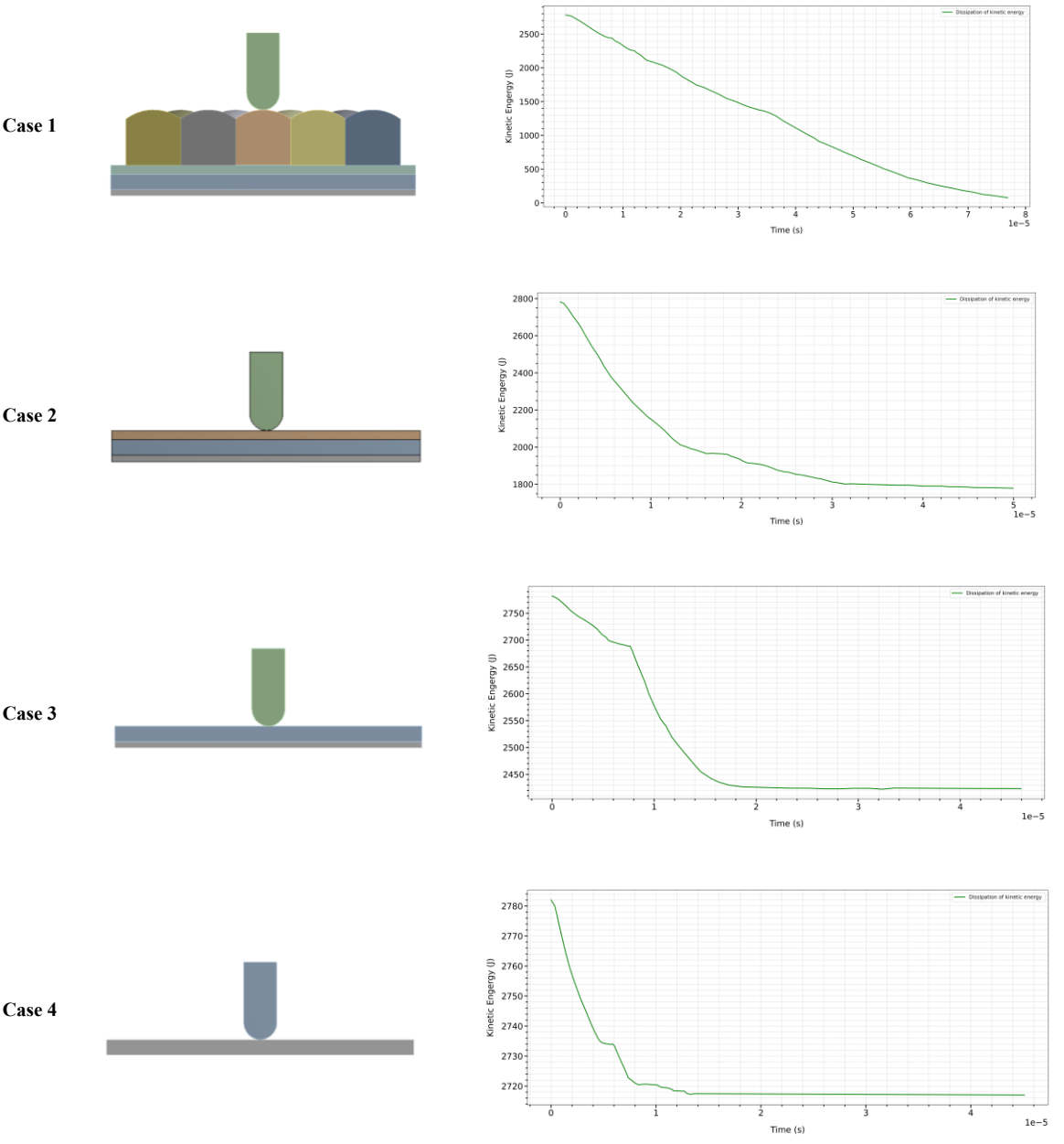

Fig. 4: Performance Analysis of Flexible Bullet Impact on Layered Protective Structures in four different cases. (**Case 1:** from the top down, bullet, ceramic cylinders, Ti6Al4V (3 mm), UHMWPE (5 mm), Ti6Al4V (2 mm); **Case 2:** from the top down, bullet, Ti6Al4V (3 mm), UHMWPE (5 mm), Ti6Al4V (2 mm); **Case 3:** from the top down, bullet, UHMWPE (5 mm), Ti6Al4V (2 mm); **Case 4:** from the top down, bullet, UHMWPE (5 mm)).

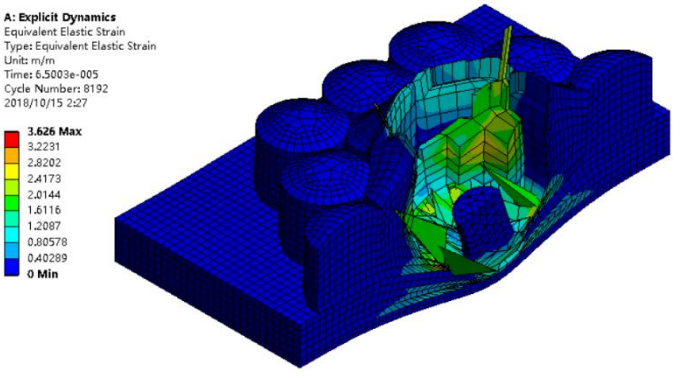

Fig. 5: Flexible projectile impact simulation.

The flexible projectile penetration profile is shown in Fig. 5, where all the boundary conditions are the same as the previous simulation, apart from the projectile being deformable. With a flexible projectile that comes to a halt before penetrating the last layer (Ti6Al4V), as it was in the real experiment, and the adjacent ceramic cylinders fractured into pieces, and so did the ceramics in the real experiment in Fig. 6.[3] The steel projectile blunted by the armor is shown in Fig. 6a, and the appearance of the eroded projectile resembles the real bullet after the impact test in Fig. 6b.[15]

3.3 Simulation of only the UHMPE (middle plate) penetration with rigid steel projectile

To interpret how the UHWMPE of 5mm in thickness reacts against the rigid projectile in Ansys, the UHWMPE layer impacted by the rigid bullet at the velocity of 818 m/s is simulated, and the penetration profile is given in Fig. 7. The energy absorption process is shown in Fig. 8. The rigid projectile penetrates the sole UHWMPE by dissipating only 116 J kinetic energy in Fig. 8.

a) b)

Fig. 6: a) Steel projectile after stopping by the armor in simulation, and b) Real bullet after the impact test.[15]

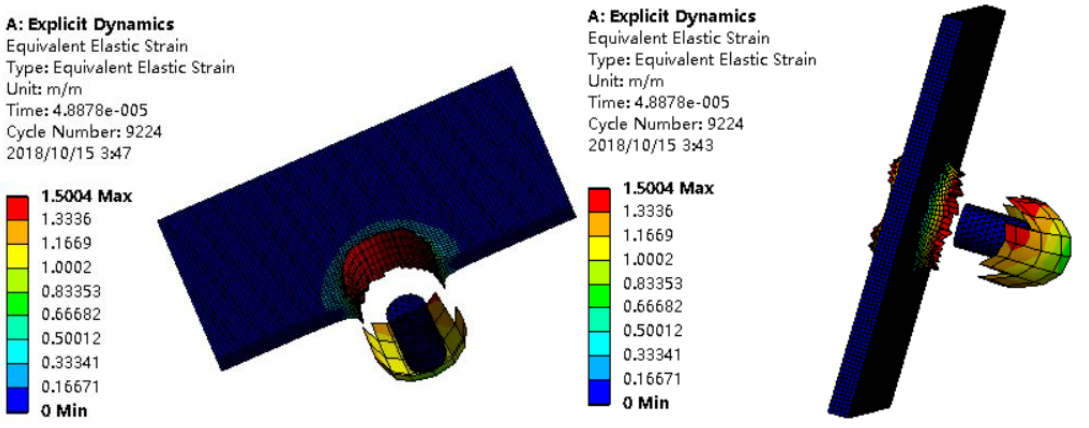

Fig. 7: Simulation of UHWMPE penetration by the rigid steel projectile.

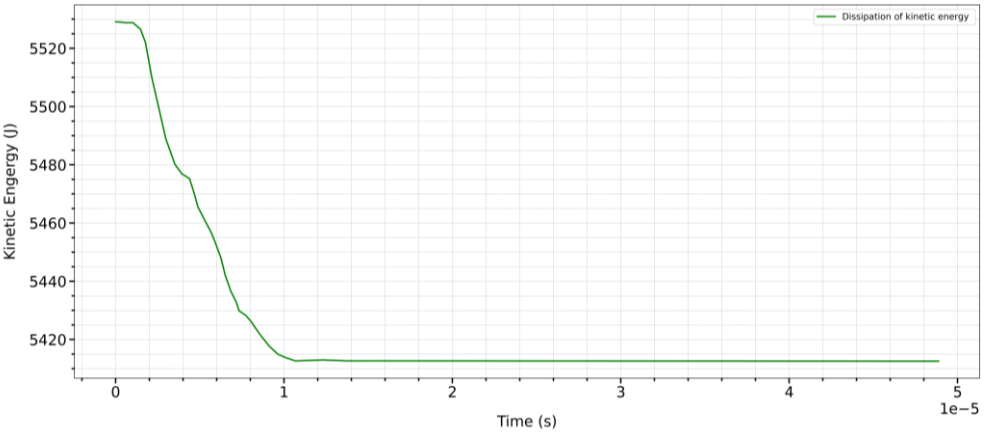

Fig. 8: Kinetic energy absorption of the projectile during the sole UHWMPE penetration.

4. Conclusion

To conclude, the simulation results of the impact test provide significant insights into the behavior of projectiles under varying conditions. It was observed that the use of a flexible projectile produces a more realistic and nuanced representation of impact dynamics when compared to a rigid projectile. This is particularly evident in its ability to more accurately reflect the deformation and energy transfer mechanisms that occur upon impact. The absence of a brass jacket, while influential in certain scenarios, does not negate the advantage of the flexible projectile in simulating realistic outcomes.

Regarding the ultra-high molecular weight polyethylene (UHMWPE) material, its standalone performance in resisting projectile impacts is notably limited. Without additional protective components, such as a covering or supporting plate, UHMWPE cannot provide significant defense against high-velocity projectiles. The material's potential for impact mitigation relies heavily on external reinforcement to distribute and absorb kinetic energy effectively.

The analysis of different layered configurations, as outlined in Cases 1 to 4, highlights the critical role of ceramic and titanium alloy components in enhancing impact resistance. In particular, Case 1 (bullet, ceramic cylinders, Ti6Al4V, UHMWPE, Ti6Al4V) demonstrated superior energy absorption due to the ceramic layer's ability to dissipate energy and the metallic plates' structural support. Case 2 (bullet, Ti6Al4V, UHMWPE, Ti6Al4V) provided considerable resistance but lacked the enhanced dissipation effects offered by the ceramic layer. Case 3 (bullet, UHMWPE, Ti6Al4V) and Case 4 (bullet, UHMWPE only) exhibited limited performance, emphasizing the necessity of multi-layered structures for adequate protection.

These findings underscore the importance of material layering and structural design in enhancing protective performance in real-world applications, particularly in defense and ballistic protection systems. Future studies integrating more advanced materials, such as hybrid composites or reactive layers, and varying projectile configurations could further refine our understanding of impact resistance mechanisms. This would significantly contribute to the development of more effective protective solutions, meeting the evolving demands of modern defense technology.

Conflict of interest

There is no conflict of interest.

Supporting Information

Not applicable.

References

[1] A. Krell, E. Strassburger, Hierarchy of key influences on the ballistic strength of opaque and transparent armor, *Advances in Ceramic Armor III*, Hoboken, NJ, USA: John Wiley & Sons, Inc., 2009, 45-55, doi: 10.1002/9780470339695.ch4.

[2] E. Medvedovski, Lightweight ceramic composite armour system, *Advances in Applied Ceramics*, 2006, **105**, 241-245, doi: 10.1179/174367606x113537.

[3] W. Liu, Z. Chen, X. Cheng, Y. Wang, A. R. Amankwa, J. Xu, Design and ballistic penetration of the ceramic composite armor, *Composites Part B: Engineering*, 2016, **84**, 33-40, doi: 10.1016/j.compositesb.2015.08.071.

[4] E. Medvedovski, Lightweight ceramic composite armour system, *Advances in Applied Ceramics*, 2006, **105**, 241-245, doi: 10.1179/174367606x113537.

[5] D. B. Rahbek, J. W. Simons, B. B. Johnsen, T. Kobayashi, D. A. Shockey, Effect of composite covering on ballistic fracture damage development in ceramic plates, *International Journal of Impact Engineering*, 2017, **99**, 58-68, doi: 10.1016/j.ijimpeng.2016.09.010.

[6] B. Li, L. Liu, X. Wang, Y. Ma, D. Pan, S. Maganti, B. Xu, Z. Guo, Effects of nano-barium sulfate on the properties of polybutylece terephthalate/polyethylene terephthalate composites, *ES Materials & Manufacturing*, 2022, **17**, 83-91, doi: 10.30919/esmm5f634.

[7] H. van der Werff, U. Heisserer, High-performance ballistic fibers, *Advanced Fibrous Composite Materials for Ballistic Protection*, Amsterdam: Elsevier, 2016, 71-107, doi: 10.1016/b978-1-78242-461-1.00003-0.

[8] W. Liu, Z. Chen, Z. Chen, X. Cheng, Y. Wang, X. Chen, J. Liu, B. Li, S. Wang, Influence of different back laminate layers on ballistic performance of ceramic composite armor, *Materials & Design*, 2015, **87**, 421-427, doi: 10.1016/j.matdes.2015.08.024.

[9] A. Zykova, A. Vorontsov, A. Chumaevskii, D. Gurianov, N. Savchenko, E. Kolubaev, S. Tarasov, Microstructures and characterization of Ti_6Al_4V alloy friction stir alloyed with Cu and Al powders, *ES Materials & Manufacturing*, 2024, **25**, 1205, doi: 10.30919/esmm1205.

[10] Q. Wang, Z. Chen, Z. Chen, Design and characteristics of hybrid composite armor subjected to projectile impact, *Materials & Design*, 2013, **46**, 634-639, doi: 10.1016/j.matdes.2012.10.052.

[11] G. A. Gogotsi, V. I. Galenko, S. P. Mudrik, B. I. Ozersky, V. V. Khvorostyany, T. A. Khristevich, Fracture resistance estimation of elastic ceramics in edge flaking: EF baseline, *Journal of the European Ceramic Society*, 2010, **30**, 1223-1228, doi: 10.1016/j.jeurceramsoc.2009.12.002.

[12] B. R. Lawn, Indentation of ceramics with spheres: a century after hertz, *Journal of the American Ceramic Society*, 1998, **81**, 1977-1994, doi: 10.1111/j.1151-2916.1998.tb02580.x.

[13] E. Medvedovski, Ballistic performance of armour ceramics: influence of design and structure. part 1, *Ceramics International*, 2010, **36**, 2103-2115, doi: 10.1016/j.ceramint.2010.05.021.

[14] M. Fejdyś, K. Kośla, A. Kucharska-Jastrząbe, M. Landwijt, Hybride composite armour systems with advanced ceramics and ultra-high molecular weight polyethylene (UHMWPE) fibres, *Fibres and Textiles in Eastern Europe*, 2016, **24**, 79-89, doi: 10.5604/12303666.1196616.

[15] D. Hu, Y. Zhang, Z. Shen, Q. Cai, Investigation on the ballistic behavior of mosaic SiC/UHMWPE composite armor

systems, *Ceramics International*, 2017, **43**, 10368-10376, doi: 10.1016/j.ceramint.2017.05.071.
[16] M. O. Yavaş, A. Avcı, M. Şımşır, A. Akdemır, Ballistic performance of Kevlar49/UHMW-PEHB26 hybrid layered-composite, *International Journal of Engineering Research and Development*, 2015, **7**, 21-27, doi: 10.29137/umagd.379789.
[17] X. Li, X. Zhang, Y. Guo, V. P. W. Shim, J. Yang, G. B. Chai, Influence of fiber type on the impact response of titanium-based fiber-metal laminates, *International Journal of Impact Engineering*, 2018, **114**, 32-42, doi: 10.1016/j.ijimpeng.2017.12.011.
[18] Y. Yu, Y. Wu, B. Wang, M. Ma, G. Gao, Review of the penetration resistance performance of lightweight ceramic composite armor under high-speed impact, *Mechanics of Advanced Materials and Structures*, 2025, **32**, 2056-2078, doi: 10.1080/15376494.2024.2374442.
[19] N. K. Naik, S. Kumar, D. Ratnaveer, M. Joshi, K. Akella, An energy-based model for ballistic impact analysis of ceramic-composite armors, *International Journal of Damage Mechanics*, 2013, **22**, 145-187, doi: 10.1177/1056789511435346.
[20] B. A. Roeder, C. T. Sun, Dynamic penetration of alumina/aluminum laminates: experiments and modeling, *International Journal of Impact Engineering*, 2001, **25**, 169-185, doi: 10.1016/S0734-743X(00)00031-2.
[21] K. Karthikeyan, B. P. Russell, N. A. Fleck, M. O'Masta, H. N. G. Wadley, V. S. Deshpande, The soft impact response of composite laminate beams, *International Journal of Impact Engineering*, 2013, **60**, 24-36, doi: 10.1016/j.ijimpeng.2013.04.002.
[22] K. Karthikeyan, B. P. Russell, N. A. Fleck, H. N. G. Wadley, V. S. Deshpande, The effect of shear strength on the ballistic response of laminated composite plates, *European Journal of Mechanics - A/Solids*, 2013, **42**, 35-53, doi: 10.1016/j.euromechsol.2013.04.002.
[23] A. Ruggiero, G. Iannitti, N. Bonora, M. Ferraro, Determination of Johnson-holmquist constitutive model parameters for fused silica, *EPJ Web of Conferences*, 2012, **26**, 04011, doi: 10.1051/epjconf/20122604011.
[24] D. Bürger, A. Rocha de Faria, S. F. M. de Almeida, F. C. L. de Melo, M. V. Donadon, Ballistic impact simulation of an armour-piercing projectile on hybrid ceramic/fiber reinforced composite armours, *International Journal of Impact Engineering*, 2012, **43**, 63-77, doi: 10.1016/j.ijimpeng.2011.12.001.
[25] M. Stopel, D. Skibicki, Determination of Johnson-Cook model constants by measurement of strain rate by optical method, *AIP Conference Proceedings*, 2016, **1780**, 060003, doi: 10.1063/1.4965956.
[26] M. Grujicic, G. Arakere, T. He, W. C. Bell, B. A. Cheeseman, C. F. Yen, B. Scott, A ballistic material model for cross-plied unidirectional ultra-high molecular-weight polyethylene fiber-reinforced armor-grade composites, *Materials Science and Engineering: A*, 2008, **498**, 231-241, doi: 10.1016/j.msea.2008.07.056.
[27] L. Chen, J. Li, Y. Zhao, M. Li, L. Li, L. Chen, H. Hou, Numerical simulation and optimization of indirect squeeze casting process, *Engineered Science*, 2021, **13**, 65-70, doi: 10.30919/es8d1157.